

## Dark sector to restore cosmological concordance

Itamar J. Allali<sup>1,2,\*</sup>, Mark P. Hertzberg<sup>1,3,†</sup>, and Fabrizio Rompineve<sup>1,2,‡</sup>

*Institute of Cosmology, Department of Physics and Astronomy, Tufts University, Medford, Massachusetts 02155, USA*



(Received 20 May 2021; accepted 27 September 2021; published 27 October 2021)

We develop a new phenomenological model that addresses current tensions between observations of the early and late Universe. Our scenario features: (i) a decaying dark energy fluid (DDE) with a transition at  $z \sim 5,000$ , to raise today's value of the Hubble parameter, and (ii) an ultralight axion (ULA), which starts oscillating at  $z \gtrsim 10^4$ , to suppress the matter power spectrum. Our Markov chain Monte Carlo analyses show that such a dark sector model fits a combination of cosmic microwave background (CMB), baryon acoustic oscillations, and Large Scale Structure (LSS) data slightly better than the  $\Lambda$ CDM model, while importantly reducing both the  $H_0$  and  $S_8$  tensions with late universe probes ( $\lesssim 3\sigma$ ). Combined with measurements from cosmic shear surveys, we find that the discrepancy on  $S_8$  is reduced to the  $1.4\sigma$  level. Adding local supernovae measurements, we find that the  $H_0$  and  $S_8$  tensions are reduced to the  $1.4\sigma$  and  $1.2\sigma$  levels respectively, with a significant improvement  $\Delta\chi^2 \simeq -18$  compared to the  $\Lambda$ CDM model. With this complete dataset, the DDE and ULA are detected at  $\simeq 4\sigma$  and  $\simeq 2\sigma$ , respectively. We discuss a possible particle physics realization of this model, with a dark confining gauge sector and its associated axion, although embedding the full details within microphysics remains an urgent open question. Our scenario will be decisively probed with future CMB and LSS surveys.

DOI: 10.1103/PhysRevD.104.L081303

### I. INTRODUCTION

Observations by the Planck satellite of the cosmic microwave background (CMB) indicate a Universe expanding today at a (Hubble) rate of  $H_0 = 67.27 \pm 0.60$  km/s/Mpc [1], assuming the  $\Lambda$  cold dark matter ( $\Lambda$ CDM) model. This is in strong ( $4.4\sigma$ ) tension with local measurements based on supernovae from the SH<sub>0</sub>ES Collaboration [2], which report a faster rate of  $H_0 = 74.03 \pm 1.42$  km/s/Mpc (see also [3]). The discrepancy between early and late Universe determinations of  $H_0$  appears to be supported by several other probes [e.g., lensing time delays [4], and baryon acoustic oscillations (BAO) and BOSS galaxy clustering data analyzed with the Effective Field Theory of LSS [5–10] (EFTofLSS)].

Further disagreement arises in the determination of the amplitude of the matter power spectrum at late times, which is often parametrized by means of the combination  $S_8 \equiv \sigma_8 \sqrt{\Omega_m/0.3}$  ( $\Omega_m$  and  $\sigma_8$  being respectively the total relic abundance of nonrelativistic matter and the variance of matter fluctuations in a sphere of radius 8 Mpc/ $h$  today). In particular, a recent combination of data from cosmic shear surveys finds  $S_8 = 0.755^{+0.019}_{-0.021}$  [11,12], in  $3.2\sigma$  tension

with the value inferred by the Planck collaboration (see also [13–17] for other measurements).

A resolution of these tensions based on systematic errors is currently lacking. It is possible that the above discrepancies may be resolved instead by modifying the cosmological ( $\Lambda$ CDM) model used to infer values of parameters from early Universe probes. A notable attempt in this direction is the addition of an early dark energy (EDE) component [18] (see also [19,20]) that is very rapidly diluted after the epoch of matter radiation equality. This scenario significantly alleviates the Hubble tension when fitted to a combination of Planck, BAO, and supernovae data, but exacerbates the  $S_8$  tension. Therefore, when cosmic shear as well as EFTofLSS data are included, the resolving power of EDE is reduced [21–25]. EDE also relies on a scalar field with a highly tuned potential [26]. A somewhat more particle-physics-oriented scenario is that of a strong first order phase transition in a weakly coupled scalar field at the eV scale, as proposed in the new early dark energy (NEDE) scenario [27–29]. However, this similarly increases the  $S_8$  tension, while other well-motivated scenarios, such as decay through resonance [26] (see also [30]) or modified gravity models (see e.g., [31–37]) struggle to provide convincing solutions.

In this paper, we propose a new phenomenological dark sector (DS) model, which is instead able to more fully restore cosmological concordance by predicting both a larger expansion rate and a suppressed matter power

\*itamar.allali@tufts.edu

†mark.hertzberg@tufts.edu

‡fabrizio.rompineve@tufts.edu

spectrum at late times. Our model features both a decaying dark energy (DDE) component, which addresses the Hubble tension similarly to the EDE and NEDE scenarios, as well as an ultralight axion (ULA) field with a standard potential and generic initial conditions. By virtue of the misalignment mechanism, this axion contributes a fraction of the relic abundance of dark matter (DM) today. However, in contrast to CDM, it causes a suppression of power on small scales, due to the scale-dependent sound speed of its perturbations [38–40], and thus addresses the  $S_8$  tension (see also [41] for a different ULA model with similar goals).

## II. PHENOMENOLOGICAL MODEL

Our DS model is composed of two ingredients:

- (1) A DDE fluid which undergoes a sharp transition at some redshift  $z_{\text{dde}}$ , after which its equation of state parameter changes from  $w = -1$  to  $w = w_f > 1/3$ .
- (2) A ULA field  $a$  with a potential of the standard form  $V = m_a^2 f_a^2 (1 - \cos a/f_a)$ , where  $m_a$  and  $f_a$  are the axion mass and decay constant, respectively.

For the DDE fluid, we adopt the effective fluid modeling put forth in the NEDE scenario of [27,28] to perform a concrete numerical analysis. This model is general enough to capture the effective behavior of several possible microscopic scenarios. Its crucial features are: At the background level, the transition at  $z_{\text{dde}}$  is assumed to occur in much less than a Hubble time, and is thus modeled as instantaneous. The redshift  $z_{\text{dde}}$  is set by a subdominant “trigger” scalar field of mass  $m_t$  once the rolling condition  $H \simeq m_t$  is satisfied. Cosmological perturbations of the DDE fluid are initially set to vanish and then are reinitialized around  $z_{\text{dde}}$  by using the perturbations of the trigger field as initial conditions. Subsequently, they are treated as those of an ideal cosmic fluid with adiabatic sound speed  $c_s^2 = w_f$ . Overall, the NEDE/DDE fluid introduces four extra parameters to the  $\Lambda$ CDM model: (i) the fraction  $F_{\text{dde}}$  of the energy density in the DDE fluid at  $z \geq z_{\text{dde}}$ , (ii) the mass of the trigger field, or equivalently, the redshift  $z_{\text{dde}}$  of the transition, (iii) the equation of state parameter  $w_f$ , and (iv) the precise value of the ratio  $H/m_t$ , at which the trigger field starts rolling. However, the latter two parameters would be fixed once a particle physics model is specified. Thus, we fix  $H/m_t = 0.2$ , justified by the dynamics of a generic scalar field. We also fix  $w_f = 2/3$ , as in [28], although our conclusions are not strongly affected by the precise value of  $w_f$ , as long as  $w_f \gtrsim 0.5$ , see also [20,28]. Overall, this leaves just two free parameters from the DDE component.

Let us now comment on the ULA component. At early times such an axion field behaves as dark energy with  $w = -1$ . Once  $H \lesssim m_a$ , the axion starts oscillating and eventually behaves as a dark matter component at late times, according to the misalignment mechanism. However, its effects on the growth of structures can deviate

crucially from those of cold DM. In a Universe where the DM is made of ULAs, subhorizon matter perturbations with wavenumbers above the axion Jeans wave number  $k_J/a = 6^{1/4} \sqrt{H m_a}$  do not grow during matter domination, but rather oscillate [38–40] (see also [42]). In a Universe where a ULA makes up a fraction  $r_a \equiv \Omega_a/\Omega_{\text{dm}}$  of the DM, it can be shown that the suppression of the matter power spectrum is roughly  $(\mathcal{P}_{a+cdm}^k / \mathcal{P}_{cdm}^k)_{k > k_{J,0}} \sim (k_{J,\text{eq}}/k)^{8(1-\gamma)}$  [42], where  $\gamma = (-1 + \sqrt{25 - 24r_a})/4$  and  $k_{J,\text{eq}}/a_0 \simeq 0.09 \text{ Mpc}^{-1} (m_a/10^{-26} \text{ eV})$  is the Jeans wave number at equality. This estimate suggests that suppression of  $\sim 7\%$  of the matter power spectrum at the scales probed by the  $S_8$  parameter can be obtained if the Universe contains an axion with  $m_a \lesssim 10^{-26} \text{ eV}$  and  $r_a \sim 0.05$ .

At the particle physics level, a ULA is fully described by the additional three parameters: (v) its mass  $m_a$ , (vi) its decay constant  $f_a$ , and (vii) its initial field value,  $\theta_i = a_i/f_a$ . However, this last parameter is most reasonably  $\mathcal{O}(1)$ , unless further tuning or model building is invoked. We choose a typical value  $\theta_i = 2$ , although the precise choice does not alter our conclusions. Once this parameter is fixed,  $m_a$  and  $f_a$  can be traded for the redshift at which axion oscillations begin,  $z_a$ , and  $r_a$ . This leaves us with two parameters from this component also.

## III. DATASETS AND RESULTS

We have numerically implemented the DS model presented in the previous section, by merging two publicly available extensions of the Boltzmann code CLASS [43]: TriggerCLASS [44], developed in [27,28] to study the NEDE scenario, and AxiCLASS [45], developed in [46,47]. This latter code uses the state-of-the-art effective fluid model of [46] to compute the cosmological implications of ULAs. We have then performed an MCMC analysis of our DS model, using the MontePython sampler [48,49] also to find the  $\chi^2$ , while we analyzed and plotted posterior distributions using GetDist [50,51].

After the choices described above, our DS model features four free parameters in addition to the six parameters of the  $\Lambda$ CDM model:  $F_{\text{dde}}$ ,  $z_{\text{dde}}$ ,  $r_a$  and  $z_a$ . In order to obtain reliable results, we find it necessary to fix the parameter  $z_a$  in the MCMC analysis (see also [46,52,53] for a similar strategy). We then choose  $z_a \simeq 10^{4.2}$ , which corresponds to  $m_a \simeq 10^{-26} \text{ eV}$ , since this alleviates cosmological tensions most significantly. We keep the remaining three parameters free to vary, and comment on how our results are affected by a different choice of  $z_a$  or by also fixing  $z_{\text{dde}}$  in (the Supplemental Material) [54]. In addition, we model neutrinos as two massless plus one massive species with  $m_\nu = 0.06 \text{ eV}$ , following the Planck collaboration.

We consider four different combinations of cosmological datasets in this work:

- (i) **P18 + BAO**: Planck 2018 high- $\ell$  and low- $\ell$  TT, TE, EE, and lensing data [1]; BAO measurements from

TABLE I. The mean (best-fit)  $\pm 1\sigma$  error of the cosmological parameters obtained by fitting our three-parameter DS model to the four cosmological datasets described in the text. The discrepancy of the inferred values of  $H_0$  and  $S_8$  (both for  $\Lambda$ CDM and for the DS model) with respect to SH<sub>0</sub>ES and the combined analysis of [11], respectively, is shown, as well as the improvement in  $\chi^2$  with respect to  $\Lambda$ CDM [using the same datasets (the Supplemental Material) [54]].

Parameter	P18 + BAO	P18 + BAO + EFT	P18 + BAO + EFT + S <sub>8</sub>	P18 + BAO + EFT + S <sub>8</sub> + SN + H <sub>0</sub>
100 $\omega_b$	2.267(2.277) <sup>+0.022</sup> <sub>-0.026</sub>	2.265(2.289) <sup>+0.020</sup> <sub>-0.027</sub>	2.274(2.28) <sup>+0.020</sup> <sub>-0.026</sub>	2.303(2.295) <sup>+0.023</sup> <sub>-0.025</sub>
$\omega_{cdm}$	0.1241(0.1261) <sup>+0.0031</sup> <sub>-0.0044</sub>	0.1227(0.127) <sup>+0.0027</sup> <sub>-0.0040</sub>	0.1191(0.12) <sup>+0.0025</sup> <sub>-0.0035</sub>	0.1235(0.1238) <sup>+0.0030</sup> <sub>-0.0029</sub>
ln 10 <sup>10</sup> A <sub>s</sub>	3.057(3.051) <sup>+0.015</sup> <sub>-0.015</sub>	3.054(3.058) <sup>+0.015</sup> <sub>-0.015</sub>	3.050(3.047) <sup>+0.015</sup> <sub>-0.015</sub>	3.062(3.057) <sup>+0.015</sup> <sub>-0.015</sub>
n <sub>s</sub>	0.9761(0.9784) <sup>+0.0074</sup> <sub>-0.0089</sub>	0.9743(0.9864) <sup>+0.0067</sup> <sub>-0.0087</sub>	0.9738(0.9748) <sup>+0.0065</sup> <sub>-0.0083</sub>	0.9860(0.9828) <sup>+0.0065</sup> <sub>-0.0066</sub>
$\tau_{reio}$	0.0565(0.0518) <sup>+0.0068</sup> <sub>-0.0075</sub>	0.0561(0.0551) <sup>+0.0068</sup> <sub>-0.0075</sub>	0.0557(0.0545) <sup>+0.0071</sup> <sub>-0.0071</sub>	0.0574(0.0562) <sup>+0.0069</sup> <sub>-0.0077</sub>
H <sub>0</sub> [ km/s/Mpc ]	69.3(69.3) <sup>+1.0</sup> <sub>-1.4</sub>	69.09(70.58) <sup>+0.86</sup> <sub>-1.4</sub>	69.37(70.02) <sup>+0.85</sup> <sub>-1.4</sub>	71.56(70.99) <sup>+0.98</sup> <sub>-0.98</sub>
F <sub>dde</sub>	<0.137[95%](0.077)	<0.124[95%](0.11)	<0.127[95%](0.073)	0.124(0.123) <sup>+0.034</sup> <sub>-0.029</sub>
z <sub>dde</sub>	5168(5452) <sup>+1100</sup> <sub>-1300</sub>	5193(5352) <sup>+1300</sup> <sub>-1600</sub>	5055(4440) <sup>+1300</sup> <sub>-1600</sub>	4749(4894) <sup>+640</sup> <sub>-820</sub>
r <sub>a</sub> ≡ Ω <sub>a</sub> /Ω <sub>dm</sub>	<0.032[95%](0.005)	<0.039[95%](0.014)	<0.069[95%](0.037)	0.048(0.052) <sup>+0.017</sup> <sub>-0.017</sub>
log <sub>10</sub> z <sub>a</sub>	Fixed to: 4.2	Fixed to: 4.2	Fixed to: 4.2	Fixed to: 4.2
m <sub>a</sub> [10 <sup>-26</sup> eV]	(1.15)	(1.15)	(1.14)	(1.15)
f <sub>a</sub> [10 <sup>16</sup> GeV]	<9.565[95%](3.816)	<10.438[95%](6.114)	<14.34[95%](9.908)	11.2(12.0) <sup>+2.4</sup> <sub>-1.9</sub>
S <sub>8</sub>	0.827(0.838) <sup>+0.016</sup> <sub>-0.013</sub>	0.820(0.826) <sup>+0.017</sup> <sub>-0.014</sub>	0.788(0.783) <sup>+0.016</sup> <sub>-0.015</sub>	0.784(0.789) <sup>+0.014</sup> <sub>-0.014</sub>
	ΛCDM	DS	ΛCDM	DS
Tension with SH <sub>0</sub> ES	4.4 $\sigma$	2.7 $\sigma$	4.3 $\sigma$	3.0 $\sigma$
Tension with S <sub>8</sub>	3.3 $\sigma$	3.1 $\sigma$	3.2 $\sigma$	2.8 $\sigma$
$\chi^2_{DS} - \chi^2_{\Lambda\text{CDM}}$	-4.0	-1.6	-7.7	-17.9

6dFGS at  $z = 0.106$  [55], SDSS MGS at  $z = 0.15$  [56] (BAO smallz), and CMASS and LOWZ galaxy samples of BOSS DR12 at  $z = 0.38, 0.51$ , and  $0.61$  [57]. For the latter, we use the “consensus” BAO + FS likelihood which also includes measurement of the growth function  $f\sigma_8(z)$  (FS) from the same samples.

- (ii) **P18 + BAO + EFT**: the datasets above with the addition of information from the full shape of the power spectrum of galaxies in the BOSS/SDDS sample, extracted by means of the EFTofLSS [8–10]. This is implemented with the publicly available PyBird code [58,59] as a combined likelihood with BAO data from the same sample.
- (iii) **P18 + BAO + EFT + S<sub>8</sub>**: the datasets above with the addition of a split-normal prior on S<sub>8</sub>, chosen according to the recent analysis of DES data in combination with KiDS/Viking [11], i.e.,  $S_8 = 0.755^{+0.019}_{-0.021}$ .
- (iv) **P18 + BAO + EFT + S<sub>8</sub> + SN + H<sub>0</sub>**: the datasets above with the addition of the Pantheon Supernovae data sample [60] (SN) and the SH<sub>0</sub>ES measurement of the Hubble parameter  $H_0 = 74.03 \pm 1.42$  km/s/Mpc [2].

Before presenting our numerical results, an important caveat on the S<sub>8</sub> prior is in order. The use of such a prior as an approximation for the full weak-lensing likelihoods has

been shown to be justified in the  $\Lambda$ CDM and EDE models [21]. For ULAs, assessing the impact of the full likelihoods requires a dedicated treatment of nonlinearities. Lacking such tools (see e.g., [61] for a discussion), we restrict our analysis to the linear power spectrum, except for nonlinearities computed in the PyBird likelihood, and assume that the use of a prior on S<sub>8</sub> correctly captures the constraints from the full DES and KiDS/Viking likelihoods on our DS model.

Our results for cosmological parameters are reported in Table I, while posterior distributions are plotted in Fig. 1. They have been obtained with at least eight chains per dataset, and  $R - 1 < 0.03$  to satisfy the Gelman-Rubin criterion [62]. Detailed model comparisons and results for the matter and temperature anisotropy power spectra are reported in (the Supplemental Material) [54]. We assess tensions by computing  $|A - B| / (\sqrt{\sigma_A^2 + \sigma_B^2})$ , where A and B ( $\sigma_{A,B}$ ) are the mean values (1 $\sigma$  errors) of  $H_0$  (or S<sub>8</sub>) inferred from the MCMC analysis and from the measurements, respectively (the Supplemental Material) [54].

Let us first comment on results obtained with the Planck + BAO dataset only: The abundances of both DS components are consistent with zero at 2 $\sigma$ , yet this dataset allows for a non-negligible fraction of the DM to be in the form of a ULA, up to  $\sim 3\%$  at 2 $\sigma$  (see [46,52] for previous similar bounds). The same is true for the DDE component, whose fraction of the total energy density at the redshift

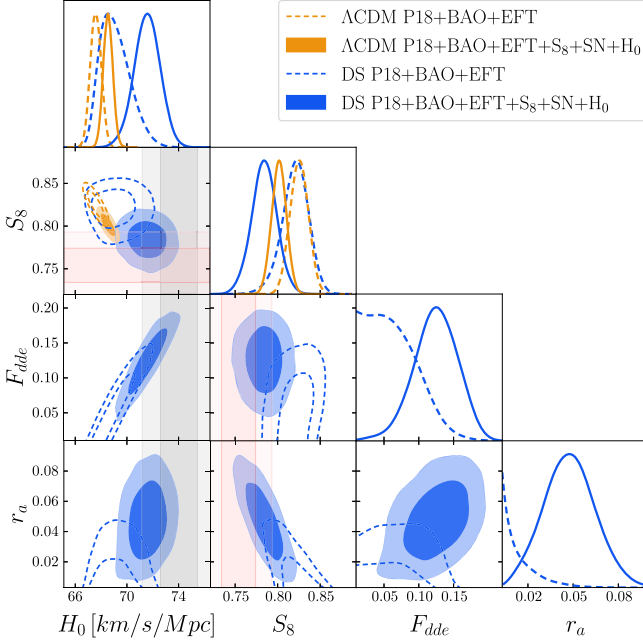


FIG. 1. Marginalized one-dimensional and two-dimensional posteriors for  $H_0$  and  $S_8$  in the  $\Lambda$ CDM and the DS models. For the latter,  $F_{\text{dde}}$  and  $r_a$  posteriors are also shown. In grey are shown the  $1\sigma$  (darker) and  $2\sigma$  (lighter) ranges for  $H_0$  from SH<sub>0</sub>ES, and similarly the  $S_8$  value from the joint analysis of [11] is shown in pink.

$z_{\text{dde}} \gtrsim 5,000$  is allowed to be as large as  $\sim 14\%$  at  $2\sigma$ , with a mild preference for  $F_{\text{dde}} \sim 7\%$ . These features lead to a significant alleviation of the  $H_0$  tension as compared to  $\Lambda$ CDM: the value of  $H_0$  inferred in the DS model is only in  $2.7\sigma$  tension with SH<sub>0</sub>ES, in contrast to  $4.4\sigma$  for  $\Lambda$ CDM. At the same time, the  $S_8$  tension is also ameliorated, albeit less dramatically. Overall, the DS model improves the fit to this dataset as compared to  $\Lambda$ CDM, although only very mildly, having  $\Delta\chi^2 \simeq -4$  with three free extra parameters. The crucial point, however, is that in the DS model, both the  $H_0$  and the  $S_8$  tensions can be interpreted as moderate statistical fluctuations, weaker than in both the  $\Lambda$ CDM and EDE/NEDE models; see also (the Supplemental Material) [54]. This conclusion is only minimally altered by the addition of the EFT likelihood, with both tensions falling to the  $3\sigma$  or below level in the combined dataset,  $\Delta\chi^2 \simeq -2$ , and the upper bound on  $r_a$  relaxed to  $4\%$ , (in agreement with [53], models with significantly lighter ULAs [41], are strongly constrained (the Supplemental Material) [54]), with a best-fit value of  $r_a \sim 1\%$ , which corresponds to  $f_a \sim 6 \times 10^{16}$  GeV. These are the first important results of this work.

It therefore seems justified to combine the Planck + BAO + EFT dataset with a prior on  $S_8$ . Very interestingly, while the DDE component is almost unaffected by this addition, we notice that the best-fit value of  $r_a$  is raised to  $\mathcal{O}(4\%)$ , while fractions up to  $\sim 7\%$  are allowed at 95% C.L., see also (the Supplemental Material) [54].

As a consequence, we obtain the second important result of this work: the tension with cosmic shear measurements is very significantly reduced to  $1.4\sigma$  level, as compared to  $2.6\sigma$  under  $\Lambda$ CDM. Notice that the  $H_0$  tension is also slightly relieved by these data, and the fit is significantly improved compared to  $\Lambda$ CDM ( $\Delta\chi^2 \simeq -8$ ). These features are in stark contrast with previous attempts to restore cosmological concordance (see [21,22] and (the Supplemental Material) [54]).

Interpreting the residual  $2.8\sigma$  tension on  $H_0$  as a moderate statistical fluctuation, it therefore seems justified to also combine the previous dataset with the local measurements from SH<sub>0</sub>ES and Pantheon. This leads to the third important result of this work, a significant improvement of the fit to data as compared to  $\Lambda$ CDM,  $\Delta\chi^2 \simeq -18$  (with three extra parameters and  $z_a$  fixed), driven mainly by a dramatically better fit to SH<sub>0</sub>ES and the  $S_8$  prior. The DDE component is now detected at  $\simeq 4\sigma$  (defined as  $4 \times$  the  $1\sigma$  interval), with a preference for  $F_{\text{dde}} \simeq 12\%$  at  $z \sim 5,000$ . The preference for the ULA component is also increased, with a vanishing relic abundance excluded at  $\simeq 2\sigma$  in the posterior distributions, and its best-fit value being  $r_a \sim 5\%$ , which corresponds to  $f_a \sim 10^{17}$  GeV, as expected from the earlier discussion of the model. These detections are the fourth important result of this work. With this combined dataset, both the  $S_8$  and  $H_0$  tensions are essentially resolved in our DS model, again in stark contrast with the  $\Lambda$ CDM and EDE/NEDE models (see (the Supplemental Material) [54] and [21–23]). Using the Akaike Information Criterion (AIC) [63] (see also [64]):  $\Delta\text{AIC} = \Delta\chi^2 + 2\Delta N$ , where  $\Delta N$  is the number of additional parameters compared to the  $\Lambda$ CDM model, we find  $\Delta\text{AIC}_{\text{DS}} = -11.9$  considering the three parameters of the DS model that we scan over in our MCMC analysis. By means of  $p = \exp(-\Delta\text{AIC}/2)$ , we find that the DS model has strong evidence over  $\Lambda$ CDM according [65].

Overall, we conclude that our DS model can restore cosmological concordance when a wide combination of early and late time datasets is considered. Importantly, both the  $S_8$  and  $H_0$  tensions remain below the  $\simeq 3\sigma$  level even when the model is confronted with early time datasets only.

#### IV. DISCUSSION

We would now like to explore whether the features of our phenomenological DS model can arise within a plausible particle physics scenario. The presence of ULAs with standard potentials is natural and appears to be a generic prediction of extra-dimensional ultraviolet (UV) theories such as String Theory, where the required  $f_a \sim 10^{17}$  GeV is a reasonable value [66,67]. These would-be massless particles get their potential from nonperturbative physics, e.g., from instantons of a gauge theory that confines at some scale  $\Lambda_c$ . In this case, the natural expectation is

$m_a \simeq \Lambda_c^2/f_a$ . The values of  $m_a$  and  $f_a$  obtained in our analysis then suggest the existence of a confining dark gauge theory with  $\Lambda_c \sim 1$  eV. For a unified model, can this gauge theory play the role of the DDE fluid? To answer this question, we need to address two separate aspects: (I) Can a confining gauge sector behave as dark energy at early times, at least sufficiently before matter-radiation equality? (II) Can it then behave as a fluid with  $w > 1/3$  below its confinement scale, at least for a sufficient amount of time after equality?

First, confining gauge sectors do indeed generically feature two very distinct behaviors in their cosmological history: On the one hand, for  $T_{\text{DS}} \gg \Lambda_c$  they are in a deconfined phase and their elementary constituents (“quarks” and “gluons”) behave as relativistic components. On the other hand, for  $T_{\text{DS}} \ll \Lambda_c$  they are in the confined phase, where massive bound states (“hadrons”) form. A PT normally occurs around the critical temperature  $T_{\text{DS},c} \lesssim \Lambda_c$ .

Very interestingly, confinement PTs can be of first order kind in several simple examples (see e.g., [68,69]), in which case they may also naturally exhibit the phenomenon of strong *supercooling*, where the PT is delayed to  $T_{\text{DS},n} \ll T_{\text{DS},c}$ . At temperatures  $T_{\text{DS},n} \lesssim T_{\text{DS}} \lesssim T_{\text{DS},c}$ , the confining sector is dominated by the vacuum energy gap between the two phases (see [69] and [70–72] for discussions in the context of strongly coupled solutions to the hierarchy problem). This can reproduce the required dark energy behavior of the DDE fluid up to sufficiently high redshifts. Further details on this possibility are provided in (the Supplemental Material) [54].

Having established that dark energy behavior is feasible at early times, we now turn to the required  $w > 1/3$  behavior at late times. The generic expectation after a first order PT is that bubble collisions lead to an initially relativistic bath of DS states. Nonetheless, the authors of [28] have argued in favor of  $w > 1/3$  after a first order PT as a consequence of subhorizon anisotropies and nonlinearities.

Here, we would like to suggest an alternative, albeit speculative, possibility. The equation of state (EoS) of a confining gauge theory can be affected by parameters beyond temperature; for instance, general arguments suggest that at very large “baryon” densities, the EoS can indeed be stiff [73], i.e.,  $c_s^2 > 1/3$  (see also [74,75] for

a discussion in the context of neutron star cores, and e.g., [76,77] for holographic models). Furthermore, a recent holographic model with a cosmological first order confinement PT and a stiff EoS below the nucleation temperature was presented in [78], where it was found that the stiffness increases as the PT becomes strongly supercooled.

Yet another strategy is to realize the DDE fluid, abandoning the connection with the ULA potential, is to make use of one or more homogeneous scalar fields that approach a near vanishing potential, thus becoming kinetically dominated, leading to  $w > 1/3$  at late times.

Whether these possibilities for  $w > 1/3$  are viable is a very interesting question for future exploration.

Finally, let us discuss further the possible constraints/signatures of our DS model. For  $m_a \sim 10^{-26}$  eV, the state-of-the-art constraint on  $r_a$  from the Lyman- $\alpha$  forest is  $r_a \leq 0.18$  at 95% C.L. [42], which is far from the  $2\sigma$  upper value obtained in our MCMC analysis. The presence of a ULA in our mass range can also affect halo formation. However, existing analyses of high- $z$  galaxies do not constrain the axion DM fraction considered in this work [79] (see also [80,81]).

However, it is anticipated that future CMB-S4 can detect a fraction of DM in a ULA with  $m_a \sim 10^{-26}$  eV at the percent level [82] (see also [83]). Future Large Scale Structure surveys, such as *Euclid* [84], DESI [85], WFIRST/Roman [86] and the Vera Rubin Observatory [87] will also further probe the existence of a DDE component. Hence upcoming observations should be able to confirm or rule out our DS model.

## ACKNOWLEDGMENTS

We would like to thank Vivian Poulin for help in setting up *AxiCLASS*, Guido D’Amico for support with *PyBird* and Evan McDonough for discussions on the  $S_8$  prior. We also thank Mark Alford for discussions on the equation of state of QCD matter in neutron stars. We thank Florian Niedermann and Martin Sloth for useful comments on a first version of this paper. We acknowledge use of Tufts HPC research cluster. The work of M. P. H. and F. R. is supported in part by National Science Foundation Grant No. PHY-2013953.

---

- [1] N. Aghanim *et al.* (Planck Collaboration), Planck 2018 results. V. CMB power spectra and likelihoods, *Astron. Astrophys.* **641**, A5 (2020).
- [2] A. G. Riess, S. Casertano, W. Yuan, L. M. Macri, and D. Scolnic, Large magellanic cloud cepheid standards

- provide a 1% foundation for the determination of the Hubble constant and stronger evidence for physics beyond  $\Lambda$ CDM, *Astrophys. J.* **876**, 85 (2019).
- [3] A. G. Riess, S. Casertano, W. Yuan, J. B. Bowers, L. Macri, J. C. Zinn, and D. Scolnic, Cosmic distances

calibrated to 1% precision with gaia EDR3 parallaxes and Hubble space telescope photometry of 75 Milky Way cepheids confirm tension with  $\Lambda$ CDM, *Astrophys. J. Lett.* **908**, L6 (2021).

[4] K. C. Wong *et al.*, H0LiCOW—XIII. A 2.4 per cent measurement of  $H_0$  from lensed quasars:  $5.3\sigma$  tension between early- and late-Universe probes, *Mon. Not. R. Astron. Soc.* **498**, 1420 (2020).

[5] D. Baumann, A. Nicolis, L. Senatore, and M. Zaldarriaga, Cosmological non-linearities as an effective fluid, *J. Cosmol. Astropart. Phys.* 07 (2012) 051.

[6] J. J. M. Carrasco, M. P. Hertzberg, and L. Senatore, The effective field theory of cosmological large scale structures, *J. High Energy Phys.* 09 (2012) 082.

[7] M. P. Hertzberg, Effective field theory of dark matter and structure formation: Semianalytical results, *Phys. Rev. D* **89**, 043521 (2014).

[8] T. Colas, G. D’Amico, L. Senatore, P. Zhang, and F. Beutler, Efficient cosmological analysis of the SDSS/BOSS data from the effective field theory of large-scale structure, *J. Cosmol. Astropart. Phys.* 06 (2020) 001.

[9] G. D’Amico, J. Gleyzes, N. Kokron, K. Markovic, L. Senatore, P. Zhang, F. Beutler, and H. Gil-Marín, The cosmological analysis of the SDSS/BOSS data from the effective field theory of large-scale structure, *J. Cosmol. Astropart. Phys.* 05 (2020) 005.

[10] M. M. Ivanov, M. Simonović, and M. Zaldarriaga, Cosmological parameters from the BOSS galaxy power spectrum, *J. Cosmol. Astropart. Phys.* 05 (2020) 042.

[11] M. Asgari *et al.*, KiDS + VIKING-450 and DES-Y1 combined: Mitigating baryon feedback uncertainty with COSEBIs, *Astron. Astrophys.* **634**, A127 (2020).

[12] S. Joudaki *et al.*, KiDS + VIKING-450 and DES-Y1 combined: Cosmology with cosmic shear, *Astron. Astrophys.* **638**, L1 (2020).

[13] C. Heymans *et al.*, CFHTLenS tomographic weak lensing cosmological parameter constraints: Mitigating the impact of intrinsic galaxy alignments, *Mon. Not. R. Astron. Soc.* **432**, 2433 (2013).

[14] H. Hildebrandt *et al.*, KiDS + VIKING-450: Cosmic shear tomography with optical and infrared data, *Astron. Astrophys.* **633**, A69 (2020).

[15] T. M. C. Abbott *et al.* (DES Collaboration), Dark energy survey year 1 results: Cosmological constraints from galaxy clustering and weak lensing, *Phys. Rev. D* **98**, 043526 (2018).

[16] C. Hikage *et al.* (HSC Collaboration), Cosmology from cosmic shear power spectra with Subaru Hyper Suprime-Cam first-year data, *Publ. Astron. Soc. Jpn.* **71**, 43 (2019).

[17] C. Heymans *et al.*, KiDS-1000 cosmology: Multi-probe weak gravitational lensing and spectroscopic galaxy clustering constraints, *Astron. Astrophys.* **646**, A140 (2021).

[18] V. Poulin, T. L. Smith, T. Karwal, and M. Kamionkowski, Early Dark Energy Can Resolve The Hubble Tension, *Phys. Rev. Lett.* **122**, 221301 (2019).

[19] P. Agrawal, F.-Y. Cyr-Racine, D. Pinner, and L. Randall, Rock ‘n’ roll solutions to the Hubble tension, [arXiv:1904.01016](https://arxiv.org/abs/1904.01016).

[20] M.-X. Lin, G. Benevento, W. Hu, and M. Raveri, Acoustic dark energy: Potential conversion of the Hubble tension, *Phys. Rev. D* **100**, 063542 (2019).

[21] J. C. Hill, E. McDonough, M. W. Toomey, and S. Alexander, Early dark energy does not restore cosmological concordance, *Phys. Rev. D* **102**, 043507 (2020).

[22] M. M. Ivanov, E. McDonough, J. C. Hill, M. Simonović, M. W. Toomey, S. Alexander, and M. Zaldarriaga, Constraining early dark energy with large-scale structure, *Phys. Rev. D* **102**, 103502 (2020).

[23] G. D’Amico, L. Senatore, P. Zhang, and H. Zheng, The Hubble tension in light of the full-shape analysis of large-scale structure data, *J. Cosmol. Astropart. Phys.* 05 (2021) 072.

[24] T. L. Smith, V. Poulin, J. L. Bernal, K. K. Boddy, M. Kamionkowski, and R. Murgia, Early dark energy is not excluded by current large-scale structure data, *Phys. Rev. D* **103**, 123542 (2021).

[25] R. Murgia, G. F. Abellán, and V. Poulin, Early dark energy resolution to the Hubble tension in light of weak lensing surveys and lensing anomalies, *Phys. Rev. D* **103**, 063502 (2021).

[26] M. Gonzalez, M. P. Hertzberg, and F. Rompineve, Ultralight scalar decay and the Hubble tension, *J. Cosmol. Astropart. Phys.* 10 (2020) 028.

[27] F. Niedermann and M. S. Sloth, New early dark energy, *Phys. Rev. D* **103**, 103537 (2021).

[28] F. Niedermann and M. S. Sloth, Resolving the Hubble tension with new early dark energy, *Phys. Rev. D* **102**, 063527 (2020).

[29] F. Niedermann and M. S. Sloth, New early dark energy is compatible with current LSS data, *Phys. Rev. D* **103**, 103537 (2021).

[30] N. Kaloper, Dark energy,  $H_0$  and weak gravity conjecture, *Int. J. Mod. Phys. D* **28**, 1944017 (2019).

[31] M.-X. Lin, M. Raveri, and W. Hu, Phenomenology of modified Gravity at recombination, *Phys. Rev. D* **99**, 043514 (2019).

[32] J. Solà Peracaula, A. Gomez-Valent, J. de Cruz Pérez, and C. Moreno-Pulido, Brans–Dicke gravity with a cosmological constant smoothes out  $\Lambda$ CDM tensions, *Astrophys. J. Lett.* **886**, L6 (2019).

[33] J. Sakstein and M. Trodden, Early Dark Energy from Massive Neutrinos as a Natural Resolution of the Hubble Tension, *Phys. Rev. Lett.* **124**, 161301 (2020).

[34] M. Zumalacarregui, Gravity in the era of equality: Towards solutions to the Hubble problem without fine-tuned initial conditions, *Phys. Rev. D* **102**, 023523 (2020).

[35] G. Ballesteros, A. Notari, and F. Rompineve, The  $H_0$  tension:  $\Delta G_N$  vs  $\Delta N_{\text{eff}}$ , *J. Cosmol. Astropart. Phys.* 11 (2020) 024.

[36] M. Braglia, M. Ballardini, W. T. Emond, F. Finelli, A. E. Gumrukcuoglu, K. Koyama, and D. Paoletti, Larger value for  $H_0$  by an evolving gravitational constant, *Phys. Rev. D* **102**, 023529 (2020).

[37] M. Braglia, M. Ballardini, F. Finelli, and K. Koyama, Early modified gravity in light of the  $H_0$  tension and LSS data, *Phys. Rev. D* **103**, 043528 (2021).

[38] M. Khlopov, B. A. Malomed, and I. B. Zeldovich, Gravitational instability of scalar fields and formation of primordial black holes, *Mon. Not. R. Astron. Soc.* **215**, 575 (1985).

[39] W. Hu, Structure formation with generalized dark matter, *Astrophys. J.* **506**, 485 (1998).

[40] J.-c. Hwang and H. Noh, Axion as a Cold Dark Matter candidate, *Phys. Lett. B* **680**, 1 (2009).

[41] L. W. Fung, L. Li, T. Liu, H. N. Luu, Y.-C. Qiu, and S. H. H. Tye, Axi-Higgs cosmology, *J. Cosmol. Astropart. Phys.* **08** (2021) 057.

[42] T. Kobayashi, R. Murgia, A. De Simone, V. Iršič, and M. Viel, Lyman- $\alpha$  constraints on ultralight scalar dark matter: Implications for the early and late universe, *Phys. Rev. D* **96**, 123514 (2017).

[43] D. Blas, J. Lesgourgues, and T. Tram, The cosmic linear anisotropy solving system (CLASS) II: Approximation schemes, *J. Cosmol. Astropart. Phys.* **07** (2011) 034.

[44] <https://github.com/flo1984/TriggerCLASS>.

[45] <https://github.com/PoulinV/AxiCLASS>.

[46] V. Poulin, T. L. Smith, D. Grin, T. Karwal, and M. Kamionkowski, Cosmological implications of ultralight axionlike fields, *Phys. Rev. D* **98**, 083525 (2018).

[47] T. L. Smith, V. Poulin, and M. A. Amin, Oscillating scalar fields and the Hubble tension: A resolution with novel signatures, *Phys. Rev. D* **101**, 063523 (2020).

[48] B. Audren, J. Lesgourgues, K. Benabed, and S. Prunet, Conservative constraints on early cosmology: An illustration of the Monte Python cosmological parameter inference code, *J. Cosmol. Astropart. Phys.* **02** (2013) 001.

[49] T. Brinckmann and J. Lesgourgues, MontePython 3: Boosted MCMC sampler and other features, *Phys. Dark Universe* **24**, 100260 (2019).

[50] A. Lewis, GetDist: A Python package for analysing Monte Carlo samples, [arXiv:1910.13970](https://arxiv.org/abs/1910.13970).

[51] <https://getdist.readthedocs.io>.

[52] R. Hložek, D. Grin, D. J. E. Marsh, and P. G. Ferreira, A search for ultralight axions using precision cosmological data, *Phys. Rev. D* **91**, 103512 (2015).

[53] A. Laguë, J. R. Bond, R. Hložek, K. K. Rogers, D. J. E. Marsh, and D. Grin, Constraining ultralight axions with galaxy surveys, [arXiv:2104.07802](https://arxiv.org/abs/2104.07802).

[54] See Supplemental Material at <http://link.aps.org/supplemental/10.1103/PhysRevD.104.L081303> for further discussions on decaying dark energy from a confining gauge theory and for detailed model comparisons.

[55] F. Beutler, C. Blake, M. Colless, D. H. Jones, L. Staveley-Smith, L. Campbell, Q. Parker, W. Saunders, and F. Watson, The 6dF galaxy survey: Baryon acoustic oscillations and the local Hubble constant, *Mon. Not. R. Astron. Soc.* **416**, 3017 (2011).

[56] A. J. Ross, L. Samushia, C. Howlett, W. J. Percival, A. Burden, and M. Manera, The clustering of the SDSS DR7 main Galaxy sample—I. A 4 per cent distance measure at  $z = 0.15$ , *Mon. Not. R. Astron. Soc.* **449**, 835 (2015).

[57] S. Alam *et al.* (BOSS Collaboration), The clustering of galaxies in the completed SDSS-III Baryon Oscillation Spectroscopic Survey: cosmological analysis of the DR12 galaxy sample, *Mon. Not. R. Astron. Soc.* **470**, 2617 (2017).

[58] G. D'Amico, L. Senatore, and P. Zhang, Limits on  $w$ CDM from the EFTofLSS with the PyBird code, *J. Cosmol. Astropart. Phys.* **01** (2021) 006.

[59] <https://github.com/pierrexyz/pybird>

[60] D. M. Scolnic *et al.*, The complete light-curve sample of spectroscopically confirmed SNe Ia from pan-STARRS1 and cosmological constraints from the combined pantheon sample, *Astrophys. J.* **859**, 101 (2018).

[61] R. Hložek, D. J. E. Marsh, D. Grin, R. Allison, J. Dunkley, and E. Calabrese, Future CMB tests of dark matter: Ultralight axions and massive neutrinos, *Phys. Rev. D* **95**, 123511 (2017).

[62] A. Gelman and D. B. Rubin, Inference from iterative simulation using multiple sequences, *Stat. Sci.* **7**, 457 (1992).

[63] H. Akaike, A new look at the statistical model identification, *IEEE Trans. Autom. Control* **19**, 716 (1974).

[64] A. R. Liddle, Information criteria for astrophysical model selection, *Mon. Not. R. Astron. Soc.* **377**, L74 (2007).

[65] R. Trotta, Bayesian methods in cosmology, [arXiv:1701.01467](https://arxiv.org/abs/1701.01467).

[66] P. Svrcek and E. Witten, Axions in string theory, *J. High Energy Phys.* **06** (2006) 051.

[67] A. Arvanitaki, S. Dimopoulos, S. Dubovsky, N. Kaloper, and J. March-Russell, String axiverse, *Phys. Rev. D* **81**, 123530 (2010).

[68] R. D. Pisarski and F. Wilczek, Remarks on the chiral phase transition in chromodynamics, *Phys. Rev. D* **29**, 338 (1984).

[69] P. Creminelli, A. Nicolis, and R. Rattazzi, Holography and the electroweak phase transition, *J. High Energy Phys.* **03** (2002) 051.

[70] B. von Harling and G. Servant, QCD-induced electroweak phase transition, *J. High Energy Phys.* **01** (2018) 159.

[71] P. Baratella, A. Pomarol, and F. Rompineve, The super-cooled Universe, *J. High Energy Phys.* **03** (2019) 100.

[72] K. Agashe, P. Du, M. Ekhterachian, S. Kumar, and R. Sundrum, Cosmological phase transition of spontaneous confinement, *J. High Energy Phys.* **05** (2020) 086.

[73] Y. B. Zel'dovich, The equation of state at ultrahigh densities and its relativistic limitations, *Sov. Phys. JETP* **14**, 1143 (1962).

[74] M. G. Alford, S. Han, and M. Prakash, Generic conditions for stable hybrid stars, *Phys. Rev. D* **88**, 083013 (2013).

[75] P. Bedaque and A. W. Steiner, Sound Velocity Bound and Neutron Stars, *Phys. Rev. Lett.* **114**, 031103 (2015).

[76] C. Hoyos, N. Jokela, D. Rodríguez Fernández, and A. Vuorinen, Breaking the sound barrier in AdS/CFT, *Phys. Rev. D* **94**, 106008 (2016).

[77] C. Ecker, C. Hoyos, N. Jokela, D. Rodríguez Fernández, and A. Vuorinen, Stiff phases in strongly coupled gauge theories with holographic duals, *J. High Energy Phys.* **11** (2017) 031.

[78] F. R. Ares, M. Hindmarsh, C. Hoyos, and N. Jokela, Gravitational waves from a holographic phase transition, *J. High Energy Phys.* **04** (2021) 100.

[79] B. Bozek, D. J. E. Marsh, J. Silk, and R. F. G. Wyse, Galaxy UV-luminosity function and reionization constraints on axion dark matter, *Mon. Not. R. Astron. Soc.* **450**, 209 (2015).

[80] D. J. E. Marsh, Axion cosmology, *Phys. Rep.* **643**, 1 (2016).

[81] B. Schwabe, M. Gosenca, C. Behrens, J. C. Niemeyer, and R. Easther, Simulating mixed fuzzy and cold dark matter, *Phys. Rev. D* **102**, 083518 (2020).

[82] K. N. Abazajian *et al.* (CMB-S4 Collaboration), CMB-S4 Science book, first edition, [arXiv:1610.02743](https://arxiv.org/abs/1610.02743).

[83] J. B. Bauer, D. J. E. Marsh, R. Hložek, H. Padmanabhan, and A. Laguë, Intensity mapping as a probe of axion dark matter, *Mon. Not. R. Astron. Soc.* **500**, 3162 (2020).

- [84] L. Amendola *et al.*, Cosmology and fundamental physics with the Euclid satellite, *Living Rev. Relativity* **21**, 2 (2018).
- [85] M. E. Levi *et al.* (DESI Collaboration), The dark energy spectroscopic instrument (DESI), [arXiv:1907.10688](https://arxiv.org/abs/1907.10688).
- [86] R. Akeson *et al.*, The wide field infrared survey telescope: 100 Hubbles for the 2020s, [arXiv:1902.05569](https://arxiv.org/abs/1902.05569).
- [87] Ž. Ivezić *et al.* (LSST Collaboration), LSST: From science drivers to reference design and anticipated data products, *Astrophys. J.* **873**, 111 (2019).